

To appear in *Astrophysical Journal*

**An Interpretation of Flat Density Cores of Clusters of Galaxies
by Degeneracy Pressure of Fermionic Dark Matter:
A Case Study of Abell 1689**

Tadashi Nakajima

*National Astronomical Observatory of Japan
Osawa 2-21-1, Mitaka, 181-8588, Japan*

and

Masahiro Morikawa

*Department of Physics, Ochanomizu University
2-1-1 Otsuka, Bunkyo, Tokyo, 112-8610, Japan*

ABSTRACT

Flat density cores have been obtained for a limited number of clusters of galaxies by strong gravitational lensing. Using a phenomenological equation of state (EOS) describing the full-to-partial degeneracy, we integrate the equation of hydrostatic equilibrium. The EOS is based on an assumption that the local kinetic energy of a classical particle induced by the gravity dissolves the quantum statistical degeneracy. The density profile is uniquely determined by four parameters, the central density, $\rho(0)$, the properties of a fermion, namely, the mass, m , and statistical weight, g , and the ratio of the total matter density and fermion density, δ . As a case study, we model the column density and 2D encircled mass profiles of A1689, whose column density profile has been observationally obtained by Broadhurst et al., using gravitational lensing. The column density and 2D encircled profiles at the core, are reasonably reproduced for models with a limited range of particle properties. In the case that previously unknown fermions with spin 1/2 dominate the dark matter, the acceptable particle mass range is between 2 and 4 eV. In the case that the dark matter consists of the mixture of degenerate relic neutrinos and classical collisionless cold dark matter particles, the mass range of neutrinos is between 1 and 2 eV, if the ratio of the two kinds of dark matter particles is fixed to its cosmic value. Both the pure fermionic dark matter models and neutrino-CDM-mixture models reproduce the observations equally well.

Subject headings: neutrinos – equation of state – dense matter – dark matter – galaxies: clusters: individual (A1689)

1. Introduction

In most of the cosmological studies, dark matter particles are treated as collisionless particles. For instance, to describe the cosmological density evolution, collisionless Boltzmann equation is adopted. In cosmological N-body simulations, a group of collisionless dark matter particles, are represented by a single collisionless particle in the computer from the coarse-grained point of view. In the treatment by the Boltzmann equation, in which the distribution function is defined in a phase space, the particle mass and statistical weight are explicitly dealt with, although the dark matter particles are still regarded as classical particles without interaction except for gravity. In the coarse-grained view adopted by N-body simulations, there is no particle information and only the global mass density distribution is obtained.

However, by adopting the assumption that dark matter particles are collisionless classical particles, we might have lost basic physics in some cases. At high number densities and relatively low temperature, low-mass elementary particles, experience quantum statistical degeneracy due to indistinguishability of identical particles. For instance, it used to be well known that the neutrino black body in the early universe was partially degenerate (Weinberg 1962). Neutrinos are fermions and the radiation pressure of the neutrino black body can be interpreted as the combination degeneracy pressure and thermal pressure. As we discuss later in this paper, massive relic neutrinos are likely to remain partially degenerate, after decoupling and even after they become nonrelativistic under adiabatic expansion.

After nonlinear evolution of a high-density part of the universe, we might see a high concentration of dark matter particles around the center of a cluster of galaxies. If dark matter particles are composed at least partially of light fermions (e.g. neutrinos), their degeneracy pressure may be large enough to support the density structure near the center of the cluster against gravity. A self-gravitating system supported by degeneracy pressure of fermions, such as a white dwarf or a neutron star, is known to have a flat-top density profile. This is our motivation to explore the possibility that recent results regarding the mass profiles of clusters of galaxies obtained by gravitational lensing (Tyson, Kochanski, & dell’Antonio 1998; Sand et al. 2002, 2004; Broadhurst et al. 2005a,b) might be explained by the degeneracy pressure of light fermionic dark matter particles.

In this paper, using a phenomenological equation of state (EOS) that describes the physical conditions between fully degenerate fermionic gas and the classical ideal gas, we integrate the equation of hydrostatic equilibrium, under the simple assumption that the local kinetic energy of a classical particle is equal to its gravitational energy determined by the 3D encircled mass. Our model is expected to be valid only near the core of a cluster where dynamical equilibrium is possibly achieved. For pure fermions, the volume density profile is uniquely determined by three parameters, the central density, $\rho(0)$, and the properties of dark matter particles, namely, the mass, m , and statistical weight, g . To compare our model with observations, we smoothly connect our model volume density profile describing the inner region to a volume density profile derived from the observed column density profile by assuming spherical symmetry at a radius near the Einstein

radius. In this way our model column density profiles can be directly compared with strong lensing results. In reality, there are baryons and possibly other forms of dark matter such as massive cold dark matter particles. These general cases are dealt with by introducing another input parameter, the ratio of the total mass density and light fermion density, δ .

A1689 studied by Broadhurst et al. (2005a,b) is the best studied cluster by both strong and weak lensing, for which column density profile is obtained from the core to radii greater than 1 Mpc. As a case study, we apply our modeling to this cluster and constrain the possible combinations of particle properties. As a natural candidate for light fermions, we consider the case of massive neutrinos.

The paper is organized as follows. We first obtain the volume density of A1689 from the observed column density profile of Broadhurst et al. (2005b) and show that eV fermions can be degenerate near the core of this cluster in §2. Our modeling procedure is described in §3 and the properties of input fermions are discussed in §4, and then the results are presented in §5. The moderate degeneracy of unbound relic neutrinos and the plausibility that they can fall into the cluster core, are discussed in §6.

2. Derivation of a Volume Density Profile of A1689 from the Column Density Profile of Broadhurst et al.

Recently Broadhurst et al. (Broadhurst et al. 2005a,b) reported a mass column density profile of the cluster of galaxies, A1689, obtained from gravitational lensing. One of the important properties of the profile is that it has a flat top. We propose that this flat-top column density profile might be explained by the effects of degeneracy pressure of fermionic dark matter. Here we analyze this proposal.

First we briefly introduce the main results of Broadhurst et al. (2005a,b). In their analysis, $1'$ corresponds to $129 \text{ kpc } h^{-1}$. In Broadhurst et al. (2005a), the central $250 \text{ kpc } h^{-1}$ in radius of multi-color HST/ACS images were analyzed. The mass column density profile, $\Sigma(r)$, is not expressed as a single power law of radius.

The mass column density profile flattens toward the center with a mean slope of $d \log \Sigma / d \log r \approx -0.55$ within $r < 250 \text{ kpc } h^{-1}$. Inside the Einstein radius ($\theta_E \approx 50''$), they obtained the slope of ≈ -0.3 from the ratio between θ_E and the radius of the radial critical curve, $\theta_r \approx 17''$. They fit their results with an inner region of an NFW profile (Navarro, Frenk & White 1996) with a relatively high concentration, $C_{vir} = 8.2$.

The mass column density, $\Sigma(r)$, is the integral of the volume density, $\rho(r)$, along the line of sight over the entire cluster scale of Mpc. In order to study the possibility of fermion degeneracy near the center of the cluster, we need information on the volume density, $\rho(r)$, instead of the column density, $\Sigma(r)$. Broadhurst et al. (2005b) present the weak-lensing analysis of the wide field

data obtained by Subaru and obtained the column density profile at $r < 2 \text{ Mpc } h^{-1}$. They fit the combined profile of HST/ACS and Subaru with an NFW profile with a very high concentration, $C_{vir} = 13.7$, significantly larger than theoretically expected value of $C_{vir} \approx 4$. They also fit the same observed column density profile with a power law profile with a core. They give this result in terms of the angular radius dependence of the convergence, κ , as

$$\kappa \propto (\theta + \theta_C)^{-n}. \quad (1)$$

$\theta_C = 1.65'$ and $n = 3.16$ give the best fit although θ_C and $n = 3.16$ are mutually dependent and a finite range of the combination (θ_C, n) gives equally good fits. In terms of χ^2 and the degrees of freedom, this core power law profile fits the observation better than the best-fit NFW profile and we use this profile for further discussion. Although Broadhurst et al. (2005b) do not claim so explicitly, the two facts that the best-fit NFW profile shows a much higher concentration than the value predicted by the CDM cosmology and the phenomenological profile, eq.(1), fits better than the best-fit NFW profile, may indicate some contradiction to the CDM cosmology.

We start our analysis from this core power-law profile, eq(1), for further discussion. We convert (1) to a column density profile, $\Sigma(r)$, in physical units of length and mass using the relations, $\kappa = \Sigma/\Sigma_{crit}$, $\Sigma_{crit} \approx 0.95 \text{ g} \cdot \text{cm}^{-2}$, and the normalization of 2D encircled mass inside the Einstein radius, r_E , $\int_0^{r_E} \Sigma(r) 2\pi r dr = \Sigma_{crit} \cdot \pi r_E^2$. The result is expressed as

$$\Sigma(r) = 25.2 \cdot (r/r_E + 2.2)^{-3.16}, \quad (\text{g} \cdot \text{cm}^{-2}) \quad (2)$$

where $r_E = 97 \text{ kpc } h^{-1}$ corresponds to $\theta_E = 45''$, the value used in Broadhurst et al. (2005b). The 2D encircled mass, $M_2(r) = \int \Sigma(r) 2\pi r dr$, is analytically obtained and $M_2(r) = 1.3 \times 10^{14} h^{-2} M_\odot$ and $1.1 \times 10^{15} h^{-2} M_\odot$ respectively for $r = r_E$ and $r = \infty$. Therefore a high concentration of the mass is expected on the scale of r_E . By assuming spherical symmetry, we wish to obtain the volume density $\rho(r)$ by solving

$$\Sigma(x) = \int \rho(\sqrt{x^2 + z^2}) dz. \quad (3)$$

Instead using a standard method like the Abel transform, we assumed another power-law profile with a core radius for $\rho(r)$ and obtained the best fit parameters, to see the changes of the core radius and the power law index. From now on, we fix $h = 0.73$ (Spergel et al. 2006), so that direct comparison between observations and models can be made. The range of integration in z is from -1.4 Mpc to $+1.4 \text{ Mpc}$, which correspond to the region with good weak lensing signals, since we need solid numbers on the scale of cluster core. The result is

$$\rho(r) = 5.1 \times 10^{-24} (r/r_E + 1.077)^{-3.41}. \quad (\text{g} \cdot \text{cm}^{-3}) \quad (4)$$

The best fit parameters somewhat depends on the range of integration. For instance, if we use the observed column density profile eq.(2) out to ± 2.8 Mpc, regardless of the strength of weak lensing signals, the core radius in units of r_E , and power-law index, change to 1.25, and -3.71, respectively. Note that the power-law index of our choice, -3.41, is closer to that of an NFW profile of -3, than -3.71. Since our interest is in the inner region as we show later, and since the contribution of the outer region to the total mass is small, our choice should be justified.

3. Modeling Procedure

3.1. Degeneracy of eV-Mass Fermions

Before proceeding to modeling of mass profiles, we first show that at the center of A1689 with volume densities of order of 10^{-24} ($\text{g}\cdot\text{cm}^{-3}$), nonrelativistic eV-mass fermions can become degenerate. Since a mass of 1 eV corresponds to 1.8×10^{-33} g, the number density, $N/V \approx 10^{11} \text{ cm}^{-3}$, and the mean inter-particle spacing is, $(N/V)^{-1/3} \approx 2 \times 10^{-4}$ cm. On the other hand, the de Broglie wavelength for a 1 eV particle with a relative velocity v is, $h/\mu_0 v = h/(\mu_0 c)(c/v) = \lambda_{Compton} \cdot (c/v) = 1.2 \times 10^{-4}(c/v)$ cm. Therefore for nonrelativistic particles with $v \ll c$, the condition for high degeneracy, $(N/V)^{-1/3} \ll \lambda_{(de\ Broglie)}$, is satisfied. We first formulate the modeling procedure of matter distribution for the case that the entire matter consists purely of fermionic dark matter and then, modify the formulation for the case that the fractional contribution of fermionic dark matter density to the total matter density is constant.

3.2. Phenomenological Equation of State

First we provide our justification for introducing an equation of state and assuming hydrostatic equilibrium for the mixture of degenerate fermions and non-degenerate classical collisionless particles. A self-gravitating system composed purely of classical collisionless particles such as cold dark matter particles may be thermodynamically anomalous (Lynden-Bell & Wood 1968) and the equation of state may be poorly defined. However, the effect of fermion degeneracy or introduction of repulsion due to Pauli's exclusion principle is to make the mixture of degenerate fermions and classical collisionless particles a thermodynamically normal system and an analysis based on hydrostatic equilibrium valid.

To deal with the general situations in which particle temperature is finite and degeneracy is partial, we need to know the equation of state (EOS), and have to determine the temperature profile along with the density profile. We adopt two major assumptions that simplify our analysis of fermionic dark matter distribution. First, we assume that the EOS, or the pressure law, has the following form,

$$p = p_D + nk_B T, \quad (5)$$

where p_D is the zero temperature degeneracy pressure given by

$$p_D = \frac{1}{5} \left(\frac{6\pi^2}{g} \right)^{2/3} \frac{\hbar^2}{m} n^{5/3}, \quad (6)$$

n is the number density and $nk_B T$ is the thermal pressure of the classical ideal gas. Eq.(5) can be rewritten as,

$$p = p_D \left(1 + \frac{5}{2} \frac{k_B T}{E_f} \right), \quad (7)$$

where E_f is the Fermi level given by

$$E_f = \left(\frac{6\pi^2}{g} \right)^{2/3} \frac{\hbar^2}{2m} n^{2/3}, \quad (8)$$

and $E_f/(k_B T)$ corresponds to the degree of degeneracy. The formulae for degeneracy pressure and Fermi level, eqs.(6,8), are derived in a textbook of statistical physics (Landau & Lifshitz 1980). This EOS, eq(5), has been used, for example, in an analytic model of the brown dwarf interior where electrons are expected to be partially degenerate (Burrows & Liebert 1993). The approximation used in this EOS may be crude for intermediate degeneracy.

The second assumption is with regard to classical kinetic energy. Collisionless particles in general may not be in local thermodynamic equilibrium at a given radius, r . As we have mentioned before, the classical thermal pressure term in eq(5) for collisionless particles is actually the pressure equivalent, $mn\sigma^2$, where σ is the velocity dispersion in the static Jeans equation with an isotropic velocity dispersion (Binney & Tremaine 1987). Physically quantum statistical degeneracy will be dissolved by classical kinetic energy, or velocity dispersion, σ , as σ increases. Here we further assume that the particle kinetic energy at r , is in balance with the gravitational energy induced by the 3D encircled mass interior to r . From this assumption, we obtain,

$$\frac{3}{2} k_B T = \frac{GmM(r)}{r}, \quad (9)$$

where

$$M(r) = \int_0^r 4\pi\rho(r)r^2 dr. \quad (10)$$

From eqs.(5,9), we obtain the expression for the pressure,

$$p = \frac{1}{5} \left(\frac{6\pi^2}{g} \right)^{2/3} \frac{\hbar^2}{m} n^{5/3} + \frac{2}{3} \frac{GmnM(r)}{r}. \quad (11)$$

3.3. Equation of Dynamical Equilibrium

For ordinary gas, the equation of hydrostatic equilibrium (EHSE) describes the dynamical equilibrium. For collisionless particles, its counterpart is the static Jeans equation with an isotropic velocity dispersion (Binney & Tremaine 1987). In the pressure law, eq(11), the first term is the gas pressure of degenerate fermions, while the second term is the pressure equivalent of collisionless non-degenerate particles. Since, the EHSE and isotropic Jeans equation exactly have the same mathematical form, eq(11) can be inserted to the EHSE,

$$\frac{dp}{dr} = -\rho(r) \frac{GM(r)}{r^2}. \quad (12)$$

Below we give a brief description of how to integrate eq(12). First, we define $N(r)$ by

$$N(r) = \int_0^r n(r)r^2 dr, \quad (13)$$

or in its differential form,

$$\frac{dN(r)}{dr} = n(r)r^2. \quad (14)$$

$N(r)$ is the 3D encircled particle number divided by 4π and satisfies a boundary condition that $N(0) = 0$.

Eq(12) is reduced to

$$\frac{dn(r)}{dr} = -\frac{[n(r)N(r) + 2r^3n(r)^2]}{[Ar^2n(r)^{2/3} + 2rN(r)]}, \quad (15)$$

where

$$A = \frac{1}{4\pi} \left(\frac{6\pi^2}{g} \right)^{2/3} \frac{\hbar^2}{Gm^3}, \quad (16)$$

which has the dimension of length. Even with double precision, the dynamic range is too large for cgs units, to deal with cluster scale quantities. We adopt kpc as the units of length. In this case, $A = 4.36 \times 10^{28}$.

Parameters that determine a solution are the central number density $n(0) = \rho(0)/m$, which is positive and finite, and particle properties, m and g . Integration of eqs.(15,14) is performed simultaneously, using the fourth-order Runge-Kutta method.

So far we have dealt with the case that the mass density is purely due to fermionic dark matter. In reality, light fermions may account for a limited fraction of entire dark matter. Moreover, the baryon-to-dark-matter ratio is about 1:5 on average for the entire universe, and we have to take into account the baryon contribution.

Since we have no reliable information on the radial dependence of $\delta = \rho(\text{total})/\rho(\text{fermion})$ near the cluster center, we assume a constant δ . By incorporating δ into eq(12), eq.(15) is modified as

$$\frac{dn(r)}{dr} = -\frac{[\delta^2 n(r)N(r) + 2\delta^2 r^3 n(r)^2]}{[Ar^2 n(r)^{2/3} + 2\delta^2 r N(r)]}. \quad (17)$$

Later we also consider the case that δ depends on r due to the contribution of a massive galaxy placed at the center to see how much model parameters are affected by the presence of a galaxy.

3.4. Applicability of the Phenomenological Equation of State

Since the asymptotic form of the phenomenological EOS is that of classical ideal gas, a model profile approaches to an isothermal profile or $\rho(r) \propto r^{-2}$ at large r , which does not approximate the behavior of the observed core-power-law profile at large r ($\rho(r) \propto r^{-3.41}$). The same is true for an NFW profile (Navarro, Frenk & White 1997) for which $\rho(r) \propto r^{-3}$ at large r . So the validity of the model is limited to the core of the cluster for which $r \sim r_E$. Therefore we cannot compare our models directly with the column density profile obtained by Broadhurst et al. (2005b), since we cannot integrate a model volume density profile along an entire line of sight. On the other hand, the most robust observable obtained from strong gravitational lensing is the 2D encircled mass within the Einstein radius, $M_2(r_E)$, which gives the best constraint on the model. The second best observable is the power-law slope of the column density profile between the radial and tangential critical curves. These two quantities are taken into account in deriving the observed density profile, but again should be taken into account in the comparison with the model as well. In any case, it is best to compare our models with the observed column density profile out to $r \sim r_E$.

3.5. Smoothly Connecting an Inner Model Profile with the Outer Observed Profile

We construct a hybrid column density profile by smoothly connecting a model volume density profile with the observed volume density profile at a transition radius r_t . The actual procedure is that the radius, r_t , is searched for at which both $\rho(r_t)$ and $d\rho/dr(r_t)$ are connected. This condition is physically justified below. We derive a model profile under the assumption of the hydrostatic equilibrium (HSE). In order for HSE to hold also at r_t , the pressure gradient, dp/dr needs to be connected as well as ρ . If the EOS has the form that the pressure p is given as an analytic function of ρ as

$$p = f(\rho), \quad (18)$$

its derivative is

$$\frac{dp}{dr} = \frac{df(\rho)}{d\rho} \frac{d\rho}{dr}. \quad (19)$$

Therefore the continuity of dp/dr is equivalent to that of $d\rho/dr$ under the condition that ρ is continuous. Since the 3D encircled mass is the volume integral of $\rho(r)$, the EHSE becomes a differential equation of second order, when the pressure is given as eq.(18). This is the mathematical justification for both ρ and $d\rho/dr$ to be connected. Our phenomenological EOS is of course analytic.

The observed profile is given as $\rho(r)$, but the validity of EHSE is not guaranteed for entire r of the cluster, since the behavior of $p(r)$ or that of the velocity dispersion $\sigma(r)$ is unknown. However in the inner region of our interest, the EHSE is expected to hold, as long as our model describes the actual physical situation.

The computation in practice is implemented as follows.

1. Give (m, g, δ) as input parameters.
2. Set the initial transition radius r_t to $0.5r_E = 66.4$ kpc. Since the location of the radial critical curve at $0.38r_E$, there is not strong observational constraint inside $0.5r_E$. In terms of the observed 2D encircled mass, $M_2(0.5r_E)$, is only 34% of the robust observable, $M_2(r_E)$.
3. Adjust $\rho(0)$ iteratively so that the agreement of the model and observed ρ s at r_t is good to 5%.
4. Increase r_t gradually until the matching of the model and observed $d\rho/drs$ becomes better than 5%, while $\rho(0)$ is continually adjusted so that the connection of $\rho(r_t)$ is maintained.
5. If the connection is found, the model and observed 2D encircled masses within r_E , $M_2(r_E)$ s are compared. When the agreement of the two encircled masses is found to be good to 2%, we accept this solution.

4. Fermion Candidates, Particle Properties, and Mass Fraction of Fermions

4.1. Particle Mass Range of Interest

Since the size of a self-gravitating degenerate star depends strongly on the particle mass as m^{-2} (Oppenheimer & Volkoff 1939), the allowed range of the particle mass is restricted to the order of eV, if the degeneracy pressure is significant only near the flat-top cluster core, whose size is order of 100 kpc. This order estimation later turns out to be correct, since solutions were found only for a narrow mass range near 1 eV. Below we examine the possible ranges of statistical weight, g , of fermions, and the fraction of the fermion density to the entire dark matter density.

4.2. Dark Matter Dominated by Unknown Weakly Interacting Fermions

From SUSY, each known boson is expected to have a fermionic superpartner. SUSY also predicts the stability of a lightest supersymmetric particle, probably the photino. However, the lack of experimental detection at energy scales less than 10 GeV, indicates that photinos are massive and are more of a candidate for cold dark matter (Peacock 1999).

Since there is no candidate predicted to exist theoretically, we simply consider the case for a particle with spin 1/2 and assume that entire dark matter consists of these unknown fermions. From the spin degrees of freedom, there are two possibilities, $g = 1$ (Majorana fermion), or $g = 2$ (Dirac fermion). Another possibility is that statistically independent particles and anti-particles equally contribute to the number density. This gives effective $g = 2$ (Majorana fermion) and $g = 4$ (Dirac fermion).

4.3. Massive Neutrinos

The most natural candidate for which its presence is well known is massive neutrinos. Due to the small mass differences ($\Delta m \leq 0.05$ eV) among the three species, they must have a similar mass (degenerate hierarchy), if the approximate particle mass is as large as 1 eV. Neutrinos and anti-neutrinos are considered as distinguishable particles and the mean number densities of relic particles are the same. It will be natural to assume that the same ratio is maintained in the cluster core, since there is no physical cause for segregation. In terms of the effective statistical weight for the three neutrino species, $g = 6$ both for Majorana and Dirac neutrinos as long as we consider light relic neutrinos. Although a Dirac particle has two helicity states, only right-handed particles were populated in the thermal equilibrium of the early universe and the current number density of left-handed particles are expected to be negligible (Lesgourgues & Pastor 2006).

The current number density of each neutrino species (particles and anti-particles) regardless of Majorana or Dirac neutrinos, is estimated to be 112.6 cm^{-3} . If we adopt the cosmological

parameters from three-year WMAP observations (Spergel et al. 2006), $h = 0.73$, $\Omega_\Lambda = 0.762$, $\Omega_{\text{DM}} = 0.196$, and $\Omega_{\text{B}} = 0.042$, where DM and B stand for dark matter and baryons respectively. The mean mass density of the three species of neutrinos with the approximate mass, m eV, is $6.018 \times 10^{-31} m \text{ g cm}^{-3}$, while the present critical density of the universe is $1.0012 \times 10^{-29} \text{ g cm}^{-3}$. Then, the neutrino mass fraction to the critical density, Ω_ν , is given by,

$$\Omega_\nu \approx 0.060m. \quad (20)$$

Near the cluster center, $R = \rho(\text{B})/\rho(\text{DM})$, can be higher than the average value due to the dissipative collapse of baryons. Since R at the cluster center is unknown, we adopt the cosmic average, $R = 0.2$, and to investigate how the change of R affects model parameters, we also model the case for $R = 0.5$. The spatial distribution of the cold dark matter and light neutrinos may also be different, if neutrino distribution is controlled by degeneracy pressure, while CDM particles behave as classical collisionless particles. This effect is neglected for our initial attempt and the $\rho(\text{DM})/\rho(\text{neutrino})$ is fixed to the cosmic value, $\Omega_{\text{DM}}/\Omega_\nu$. With these assumptions, the total mass density to neutrino mass density, δ , is related to R as,

$$\delta = (1 + R) \frac{\Omega_{\text{DM}}}{\Omega_\nu} = (1 + R) \frac{0.196}{0.060m} = (1 + R) \frac{3.26}{m}. \quad (21)$$

4.4. Effect of a Massive Galaxy

Although the total mass of galaxies in the cluster will be a small fraction of the total mass of the cluster, a massive galaxy can affect the local mass density significantly. To study the influence of a massive galaxy on model parameters, we add a toy galaxy placed at the center to the particle density and solve EHSE, and compare the result with that without this hypothetical galaxy.

For simplicity, the density profile of this galaxy is assumed to be given by a 3D Gaussian as,

$$\rho_g(r) = \rho_{g0} \exp\left(-\frac{r^2}{2r_g^2}\right), \quad (22)$$

where

$$\rho_{g0} = \sqrt{\frac{2}{\pi}} \frac{M_g}{4\pi r_g^3}, \quad (23)$$

where M_g is the mass of the galaxy and r_g is the Gaussian scale length. In modeling, δ is no longer a constant and depends on r as,

$$\delta(r) = \frac{\rho_g(r)}{\rho(\text{fermion})} + \delta(\text{particle only}). \quad (24)$$

5. Results

5.1. Dark Matter Dominated by a Single Species of Fermions

Successful solutions are listed in Table 1. The general trend is that for the same g , the smaller the particle mass, m , the larger the transition radius, r_t . If we measure the significance of a model by the radial coverage, which also corresponds the largest encircled mass coverage, the smallest m solution is the most important for a given g . For the smallest mass solutions, the range of particle mass is $m = 3.9 \sim 2.7$ eV for $g = 1 \sim 4$ for the cosmic baryon-DM ratio of 0.2. A larger baryon fraction reduces the particle mass. For the smallest m solutions, resultant volume- and column density profiles are almost identical as shown in Figs.1 and 3. There are some deficiencies of mass densities inside the location of the radial critical curve, r_c . However, in 3D and 2D encircled mass profiles shown in Figs.2 and 4, these mass deficiencies, which amount to at most 2% of the 3D encircled mass inside r_E ($2 \times 10^{12} M_\odot$), are not noticeable.

5.2. Dark Matter Consisting of Massive Neutrinos and Cold Dark Matter

The maximum allowed particle mass, m , is obtained by equating Ω_ν and Ω_{DM} as 3.27 eV. As can be seen in Table 2, successful solutions have smaller particle masses. Therefore we are dealing with the cases that dark matter consists of neutrinos and another form of particles, possibly, nondegenerate cold dark matter particles. The volume and column density profiles are given in Figs.5 and 7 respectively. Again the model profiles are always lower than the observed profile near the center. However, the discrepancy between the models and observation is negligible in the linear plots of the encircled masses shown in Figs.6 and 8. Although m depends on the baryon-DM ratio, R , the resultant profiles are essentially identical and they are not distinguishable from the general fermion cases. For $R = 0.2$ and 0.5, the smallest mass solutions are for $m = 1.6$ and 1.1 eV respectively.

5.3. Effect of a Toy Massive Galaxy on Density Profiles

It is typical to have a small fraction ($<2\%$) of deficiency in the model 3D encircled mass inside r_E ($1.06 \times 10^{14} M_\odot$). A brightest cluster galaxy at the center of a cluster, typically has a stellar mass in excess of $10^{12} M_\odot$ and a 2% deficiency may be accounted for by a single massive galaxy at the center. Since the mass profile obtained by Broadhurst et al. (2005b) includes the contribution of galaxies, we should at least examine the possible effect to our models dealing solely with particles.

Our toy galaxy has a total mass of $2 \times 10^{12} M_{\odot}$ and a Gaussian volume profile with the scale length of 20 kpc. We did not perform any fitting or adjustment of the galaxy model parameters, except that the total mass corresponds to the 3D encircled mass deficiency with respect to the observed value. It turned out that this toy galaxy had no effect on the particle mass, m , although the EHSE was solved from the origin as usual. On the other hand, as can be seen in the volume- and column densities in Figs.5 and 7, the model galaxy remedies the local mass deficiency problem at the center. In Fig.9, the Fermi levels E_F and classical kinetic energies E_K are plotted for the models without and with the toy galaxy. The toy galaxy acts as an external gravity source, whose effect on the 3D encircled mass is largest near the center. The gravity of the galaxy enhances the classical kinetic energy of a particle and dissolves the degeneracy. This is the reason why there is a dip of the Fermi level in the model with the galaxy. In other words, the EOS is softened locally by the stellar mass of the galaxy. It should be emphasized that this is true only if the galaxy is given as an external mass source unaffected by the dark matter distribution. Also this effect is pronounced only near the origin of spherical symmetry, where the fractional contribution of the galaxy to the 3D encircled mass is the greatest.

6. Discussion

6.1. Relic Neutrinos and Bound Neutrinos in the Cluster

One may wonder how fermions at the cluster center could be degenerate. Here we first point out the fact that even relic neutrinos are moderately degenerate, which used to be well known (Weinberg 1962), but appears to be forgotten lately. There is a clear distinction between the black body of fermions and that of bosons. While the range of values of the Fermi distribution function for one-particle state is between 0 and 1, that of the Bose distribution function is between 0 and ∞ . So the fermion black body is partially degenerate, while the boson black body is not. Here we calculate the degree of degeneracy for relic neutrinos immediately after decoupling and that after they become nonrelativistic, under the assumption of adiabatic expansion.

The current cosmology assumes that there are the equal numbers of neutrinos and anti-neutrinos for each species. So the present number density of each quantum statistically independent species, $n(0)$, is $112.6/2 = 56.3 \text{ cm}^{-3}$. At redshift z , the number density $n(z)$ is given by

$$n(z) = 56.3(1+z)^3 \quad (\text{cm}^{-3}). \quad (25)$$

Immediately after neutrino decoupling, when neutrinos were extremely relativistic, the Fermi level, E_f is given by

$$E_f = c [6\pi^2 \hbar^3 n(z)]^{1/3} = 2.94 \times 10^{-4} (1+z) \quad (\text{eV}). \quad (26)$$

On the other hand, the neutrino temperature then was

$$T_\nu = 1.95(1 + z) \quad (\text{K}). \quad (27)$$

Therefore the degree of degeneracy is given by

$$\frac{E_f}{k_B T_\nu} = 1.75, \quad (28)$$

which indicates moderate degeneracy. Under adiabatic expansion, this degree of degeneracy is unlikely to change, while neutrinos are relativistic. There is a transition from the relativistic to nonrelativistic regime when $k_B T = mc^2$.

Below

$$T_\nu = T_{tr} = \frac{mc^2}{k_B} = 1.16m \times 10^4 \quad (\text{K}), \quad (29)$$

or at $z_{tr} \approx 6m \times 10^3$, where m is units of eV, neutrinos become nonrelativistic. Then the expressions for both Fermi level and neutrino temperature change, but they have the same dependence on $(1 + z)$. As long as local gravity is negligible, nonrelativistic adiabatic expansion is assumed below T_{tr} ,

$$E_f = \frac{\hbar^2}{2m} [6\pi^2 n(z)]^{2/3} = 4.3 \times 10^{-8} m^{-1} (1 + z)^2 \quad (\text{eV}), \quad (30)$$

and

$$T_\nu = T_{tr} \left(\frac{1 + z}{1 + z_{tr}} \right)^2 = 3.3 \times 10^{-4} m^{-1} (1 + z)^2 \quad (\text{K}), \quad (31)$$

or

$$k_B T_\nu = 2.8 \times 10^{-8} m^{-1} (1 + z)^2 \quad (\text{eV}). \quad (32)$$

So the degree of degeneracy is

$$\frac{E_f}{k_B T_\nu} = 1.53. \quad (33)$$

Note that there is an offset of the zero point between the relativistic and nonrelativistic Fermi levels given by $E_f(\text{relativistic}) = E_f(\text{nonrelativistic}) + mc^2$, where the offset is negligible when

particles are extremely relativistic. Again in the nonrelativistic regime, relic neutrinos are expected to be moderately degenerate. Due to the change of dispersion relation of individual particles caused by the relativistic-to-nonrelativistic transition, the degree of degeneracy changes slightly, but this effect appears minor.

Next we compare the kinetic energy level of bound neutrinos in the cluster and that of unbound neutrinos to see if relic neutrinos are cold enough so that they can fall to the cluster. The Fermi level and gravitationally induced kinetic energy at the cluster core are of 10^{-4} eV or above as seen in Fig.9. On the other hand, unbound relic neutrinos which undergo adiabatic expansion have the temperature given by eq(31). For A1689 at $z = 0.18$ and for $m = 1.6$ eV, the kinetic energy of unbound relics will be 3.65×10^{-8} eV, which is well below the energy level of the particles in the cluster core. So it is possible that the relic neutrinos can fall into the cluster core.

The cluster also has hot plasma, which may affect the fermion degeneracy. Here we briefly argue that the effect of hot plasma will be minor. First of all, hot plasma and neutrinos (or weakly interacting fermions in general) interact only through gravity and the plasma temperature has nothing to do with the velocity dispersion of neutrinos, which is determined by the encircled mass at a given r . What matters is the plasma's contribution to the encircled mass (or encircled gravitational energy if the plasma is relativistic). The ratio of gas mass and total mass has been estimated to be about 7% by X-ray observations (Anderson & Madejski 2004). They interact with fermions only through Newtonian gravity, because the plasma is not hot enough to be relativistic or the kinetic energy of a plasma particle is negligible compared to the rest-mass energy. Therefore unless the plasma particles have exceptionally high concentration near the 3D center of the cluster, their effect on the encircled mass should be minor compared to that by the dark matter particles. However, an extreme high concentration is not expected unless the plasma temperature profile has a singularity near the center. Since the X-ray emission is integrated along the light of sight, X-ray observations alone will not be capable of pin-pointing the plasma temperature near the 3D center of the cluster.

6.2. Direction of the Future Study

This degenerate fermion/neutrino hypothesis should be tested observationally with future-coming density profiles of other clusters obtained by gravitational lensing. Those profiles should be modeled by the fixed set of particle properties, (m, g) , and by a varied set of the central density, $\rho(0)$. Modeling multiple cluster profiles may further constrain the particle properties.

There may be a room for improvement in the phenomenological equation of state (PEOS). The PEOS used in this paper, eq(5), overestimates the degeneracy pressure, p_D , since p_D here is the zero-temperature degeneracy pressure for a given number density, n , regardless of the temperature of fermions or regardless of the degree of degeneracy. For the same observed density profile, the best-fit model with a more realistic PEOS will require a higher number density, n , or a lower particle

mass. Another possible improvement is that without fixing the density ratio of total matter and light fermions, the densities of light fermions and collisionless cold dark matter particles can be treated separately in terms of the equation of hydrostatic equilibrium for the former and the Jean equation for the latter, while they are coupled through the total encircled mass and the common velocity dispersion at a given r .

One cosmological subject related particularly to the degeneracy of relic massive neutrinos, is its potential effect on “free streaming”. Relic neutrinos are hot dark matter, which were relativistic, when they decoupled. From the picture of completely collisionless particles, it is considered that small-scale fluctuations in the primordial neutrino density fluctuation spectrum should have been wiped out. However, the partial degeneracy of relic neutrinos implies that not all of them could have behaved as free particles. It is conceivable that the effect of Fermi-Dirac degeneracy is to suppress the “free streaming” or to preserve the initial fluctuation spectrum. Depending on the degree of this “free-streaming suppression” of neutrinos or fermionic hot dark matter in general, our expectation on the initial density fluctuation spectrum may need to be revised. We plan to investigate this potential effect quantitatively in the near future.

7. Concluding Remark

In this paper, we have shown that the observed mass profile at the center of the cluster of galaxies, A1689, is reproduced by models assuming the presence of degenerate fermionic dark matter. In the case that previously unknown fermions with spin 1/2 dominate the dark matter, the acceptable particle mass range is between 2 and 4 eV. In the case that the dark matter consists of the mixture of the degenerate relic neutrinos and classical collisionless cold dark matter particles, the mass range of neutrinos is between 1 and 2 eV, if the ratio of the two kinds of dark matter particles is fixed to its cosmic value. Both the pure fermionic dark matter models and neutrino-CDM-mixture models reproduce the observations equally well.

We thank the anonymous referee for useful comments. This study was motivated by a very interesting talk given by Tom Broadhurst in 2004 at NAOJ, Mitaka, Japan.

REFERENCES

- Anderson, K.E. & Madejski, G. M. 2004, ApJ, 607, 190
- Binney, J. & Tremaine, S. 1987, Galactic Dynamics, Princeton U. Press.
- Burrows, A. & Liebert, J. 1993, Rev. of Mod. Phys., 65, 301
- Broadhurst, T. B. et al. 2005a, ApJ, 621, 53

- Broadhurst, T. B. et al., 2005b, *ApJ*, 619, L143
- Fukushige, T., Kawai, A. & Makino, J. 2004, *ApJ*, 606, 625
- Landau L.D. & Lifshitz, E. M., 1980, *Statistical Physics*, 3rd Ed.
- Lesgourgues, J. & Pastor, S. 2006, *Phys. Rep.* 429, 307
- Lynden-Bell, D. & Wood, R. 1968, *MNRAS*, 138, 495
- Moore, B., Quinn, T., Governato, F., Statal, J., & Lake, G. 1999, 310, 1147
- Navarro, J. F., Frenk, C. S., & White, D. M. 1996, *ApJ*, 462, 563
- Navarro, J. F., Frenk, C. S., & White, D. M. 1997, *ApJ*, 490, 493
- Oppenheimer, J. R. & Volkoff, G. M. 1939, *Phys. Rev.* 55, 374
- Peacock, J. A. 1999, *Cosmological Physics*, Cambridge U. Press.
- Peebles, P. J. E. 1973, *ApJ*, 180, 1
- Sand, D. J., Treu, T. & Ellis, R. S. 2002, *ApJ*, 574, L129
- Sand, D. J., Treu, T., Smith, G. P., & Ellis, R. 2004, *ApJ*, 604, 88
- Spergel, D. N. et al. 2006, submitted to *ApJ*. astro-ph/0603449
- Tyson, J. A., Kochanski, G. P., & dell'Antonio, I. P. 1998, *ApJ*, 498, L107
- Weinberg, S. 1962, *Phys. Rev.* 128, 1457

Table 1: Solutions for a Single Species of Spin 1/2 Fermions as the Dominant Dark Matter

$\rho(B)/\rho(DM)$	Particle Type	g	(m, r_t) eV,kpc	Profile
0.2	Majorana (p)	1	(3.9,104) \sim (4.3,73)	B
	Dirac (p) or Majorana (p+ \bar{p})	2	(3.3,93) \sim (3.6,70)	I
	Dirac (p+ \bar{p})	4	(2.8,100) \sim (3.1,73)	A
0.5	Majorana (p)	1	(3.4,100) \sim (3.7,73)	A
	Dirac (p) or Majorana (p+ \bar{p})	2	(2.9,106) \sim (3.1,73)	I
	Dirac (p+ \bar{p})	4	(2.4,100) \sim (2.6,73)	A

Table 2: Solutions for the Mixture of Neutrinos and Nondegenerate Cold Dark Matter

$\rho(B)/\rho(\text{DM})$	Particle Type	g	(m, r_t) eV,kpc
0.2	$\nu + \bar{\nu}$	6	(1.6,106) \sim (2.1,73)
0.5	$\nu + \bar{\nu}$	6	(1.1,106) \sim (2.4,73)

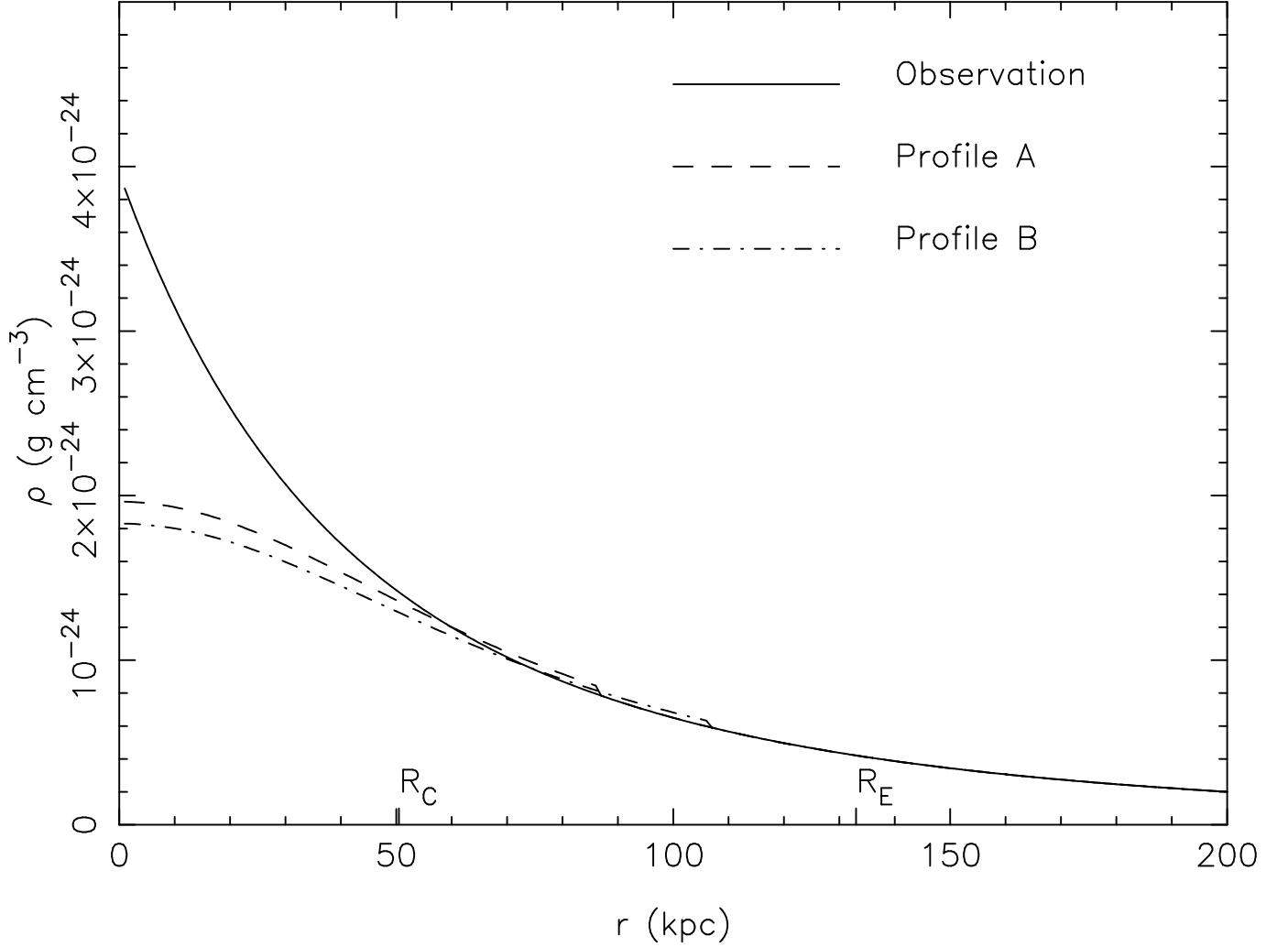


Fig. 1.— Volume density profiles for general fermionic dark matter. Profile A corresponds to the highest density model and profile B is the lowest density model and other model profiles lie between the two extremes (Profile I). The correspondence between a model profile and a solution is given in Table 1. The model profiles reproduces the observed profile well at $r > 50$ kpc. r_c and r_E stand for the radius of radial tangential critical curve and the Einstein radius respectively.

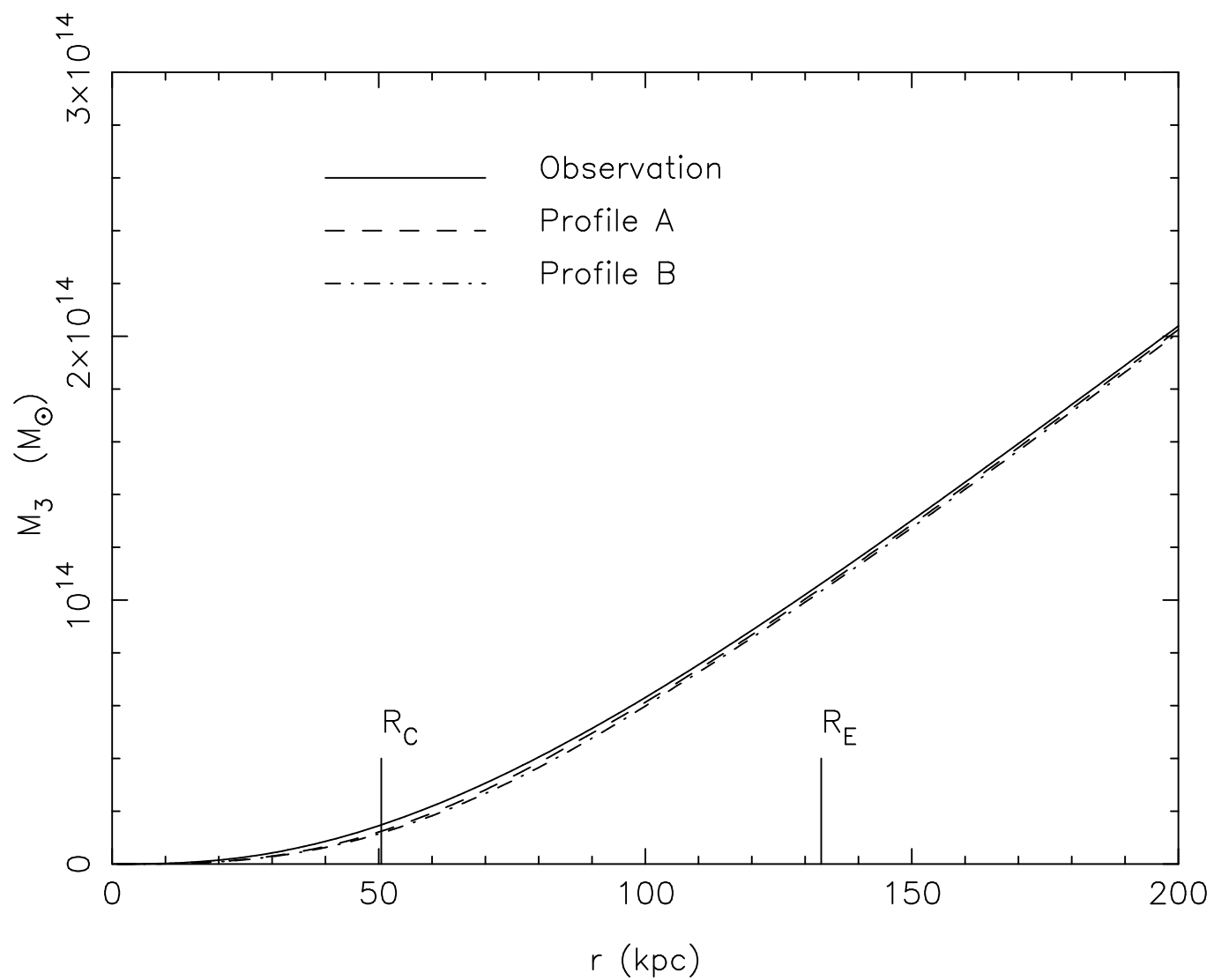


Fig. 2.— 3D encircled mass profiles for general fermionic dark matter. The observed profile and profiles A and B are indistinguishable.

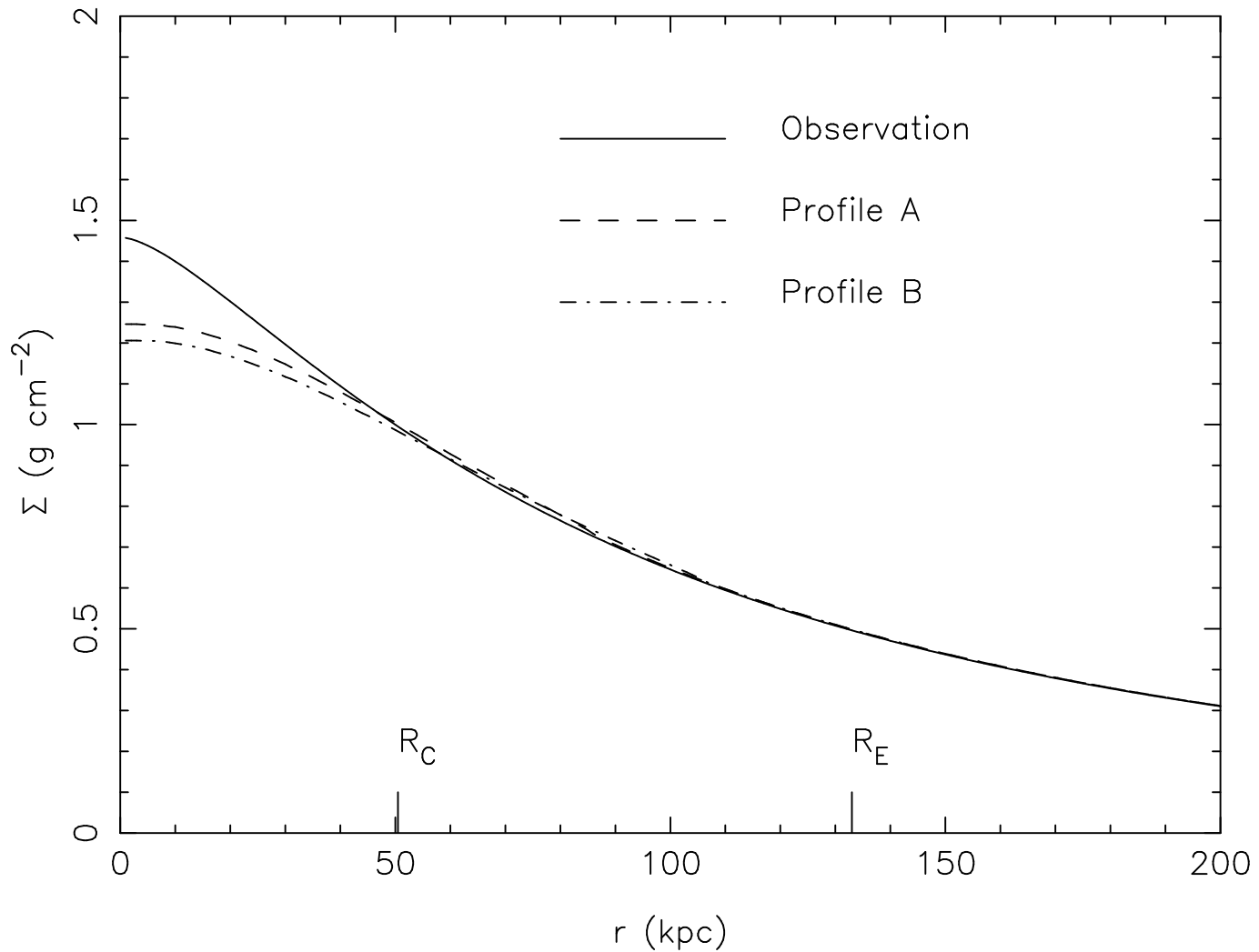


Fig. 3.— Column density profiles for general fermionic dark matter. The model profiles reproduces the observed profile well at $r > 50$ kpc.

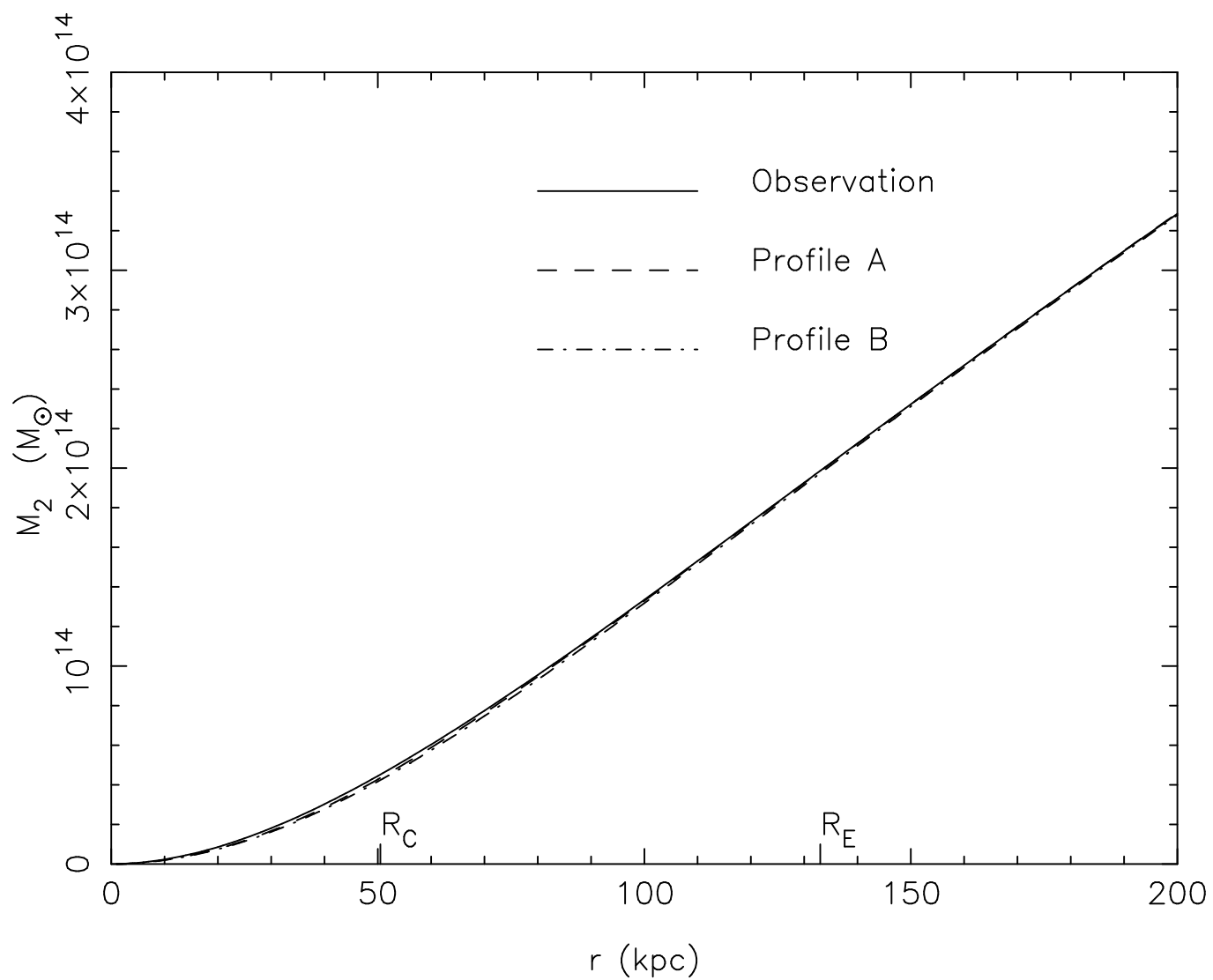


Fig. 4.— 2D encircled mass profiles for general fermionic dark matter. The observed profile and profiles A and B are indistinguishable.

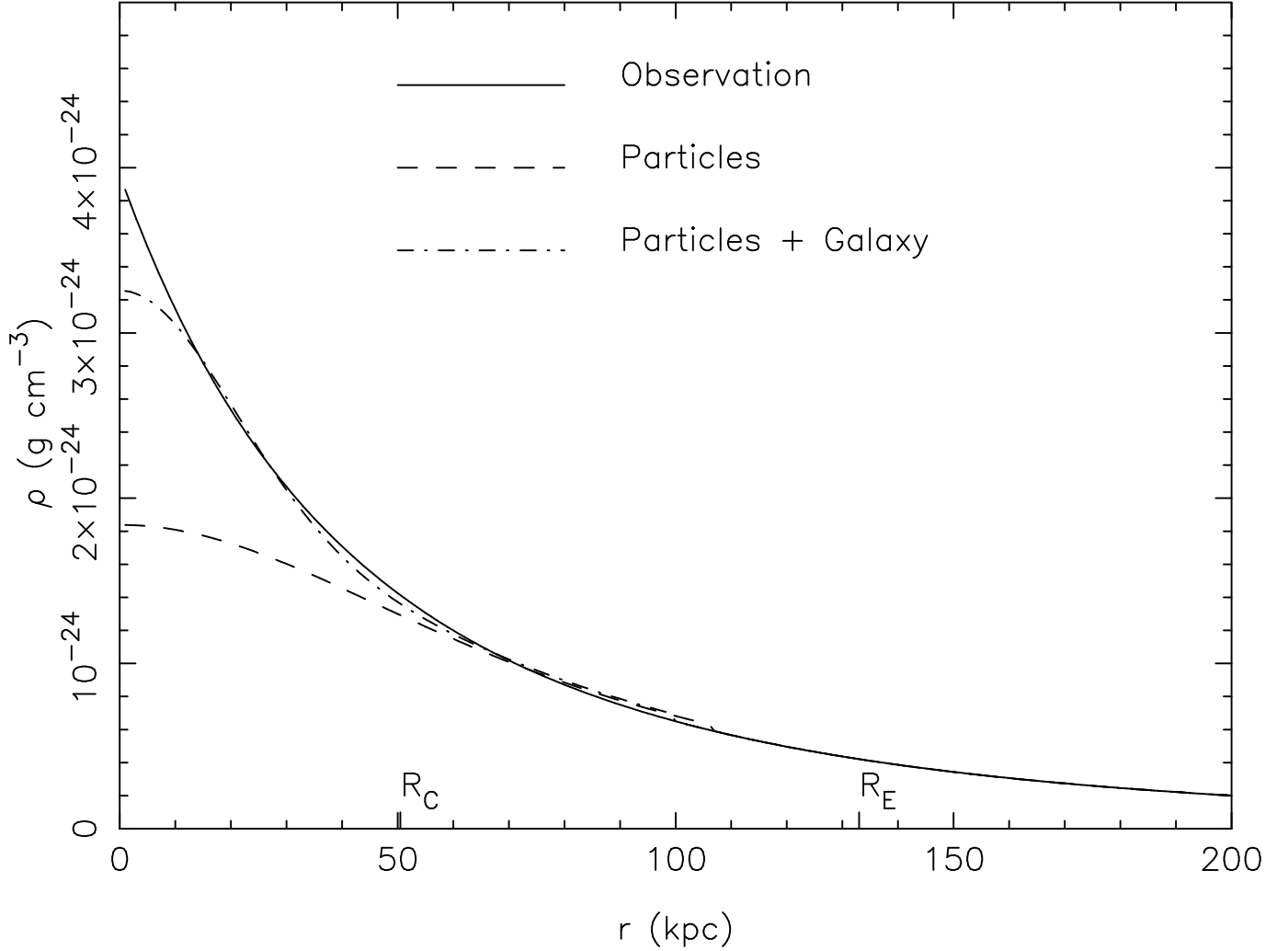


Fig. 5.— Volume density profiles for massive neutrino models. The solutions for neutrinos listed in Table 2 have almost identical mass profiles. The observed profile is compared with the representative neutrino solution (Particles = neutrinos + CDM particles + baryons) and a solution with a toy galaxy (Particle + galaxy) placed at the center. The mass of the toy galaxy is $2 \times 10^{12} M_{\odot}$, 2% of the 3D encircled mass within the Einstein radius. The model without the galaxy reproduces the observation well except for the central region, while the toy galaxy remedies the discrepancy. It should be noted that the contribution of galaxies is included in the observed density profile of Broadhurst et al. (2005b).

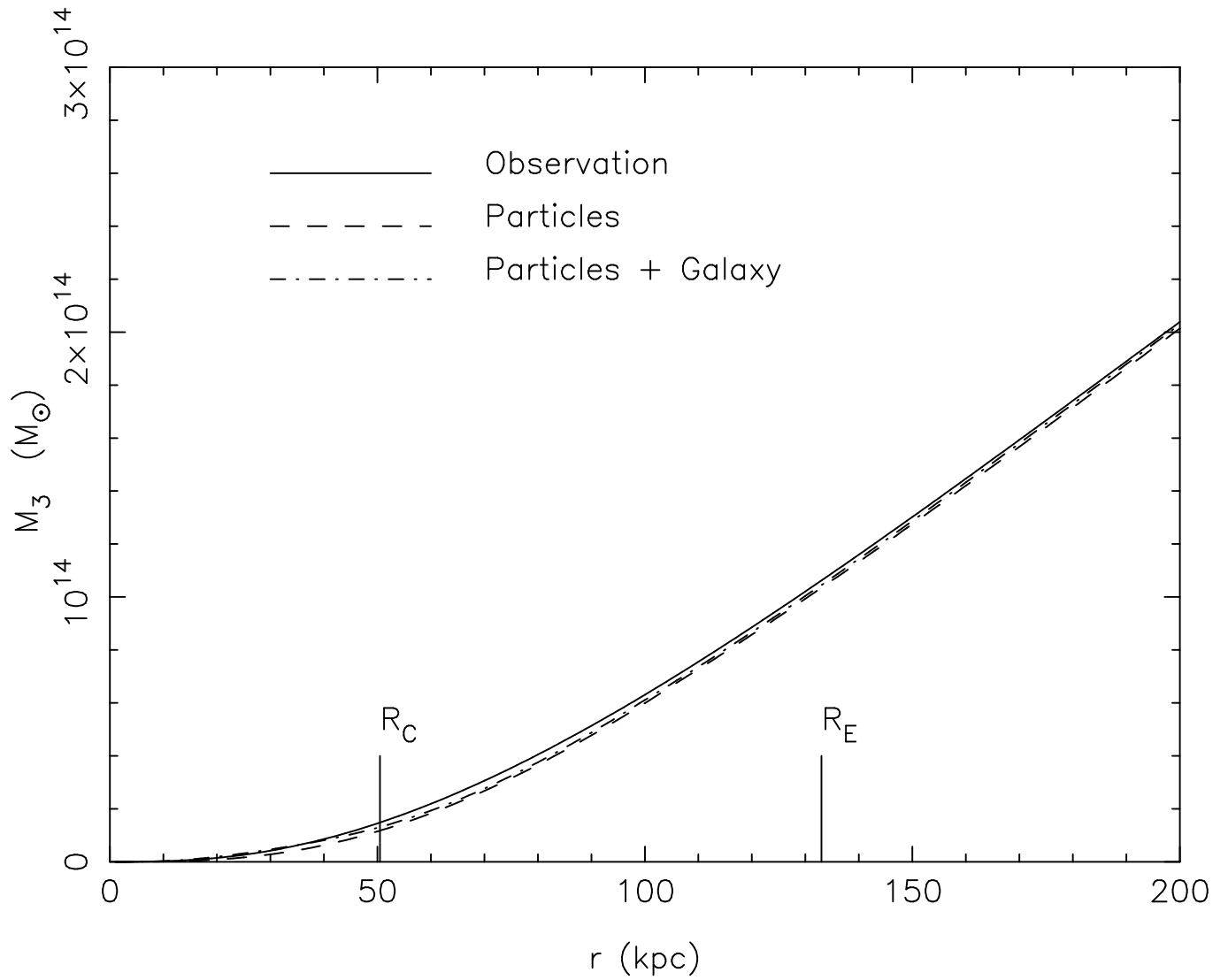


Fig. 6.— 3D encircled mass profiles for massive neutrinos models. All three profiles are indistinguishable and the effect of the central galaxy is not noticeable.

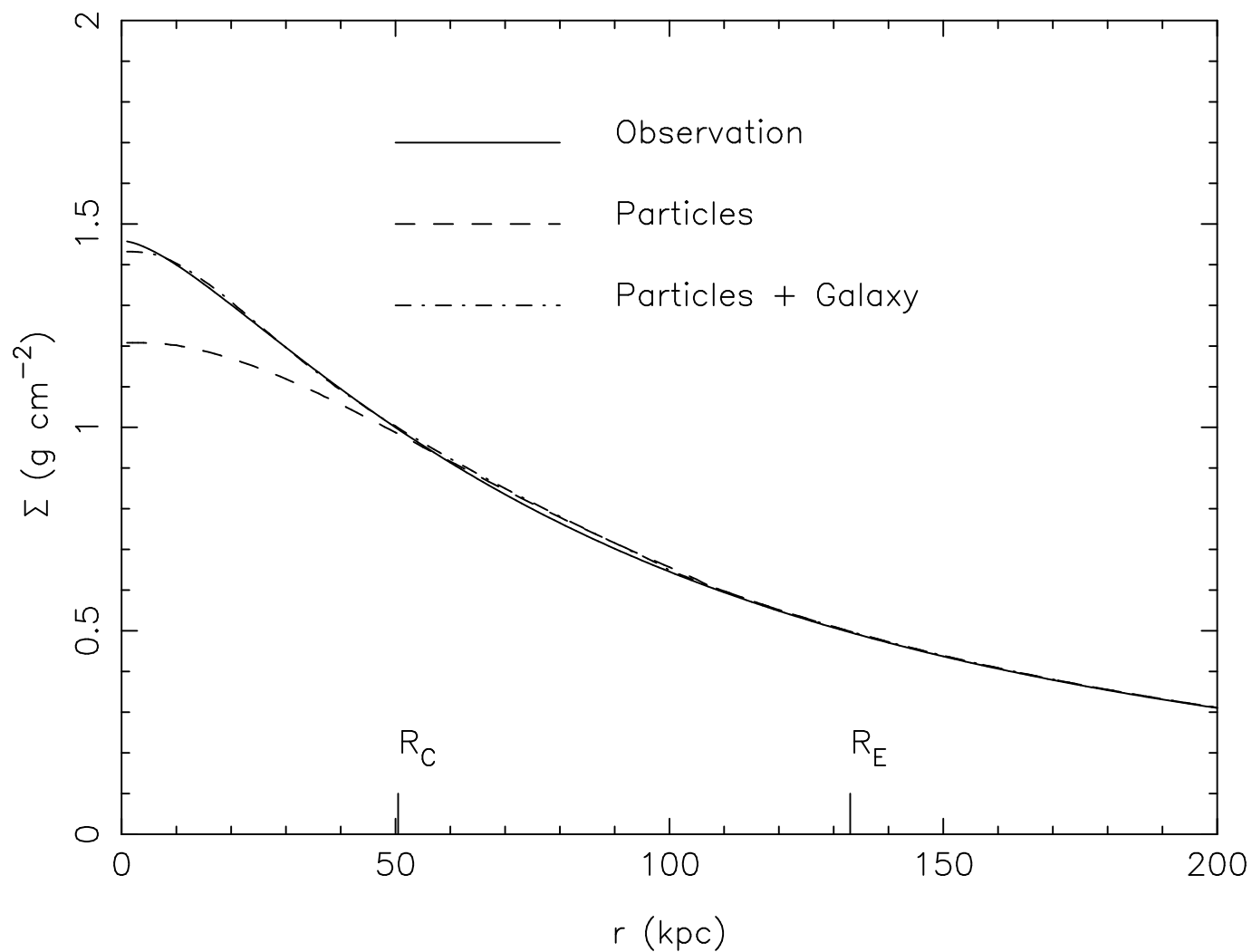


Fig. 7.— Column density profiles for massive neutrinos. Apart from the central region where the encircled mass is small, The observed profile and the representative neutrino model profile agree well. Again the toy galaxy fixes the discrepancy.

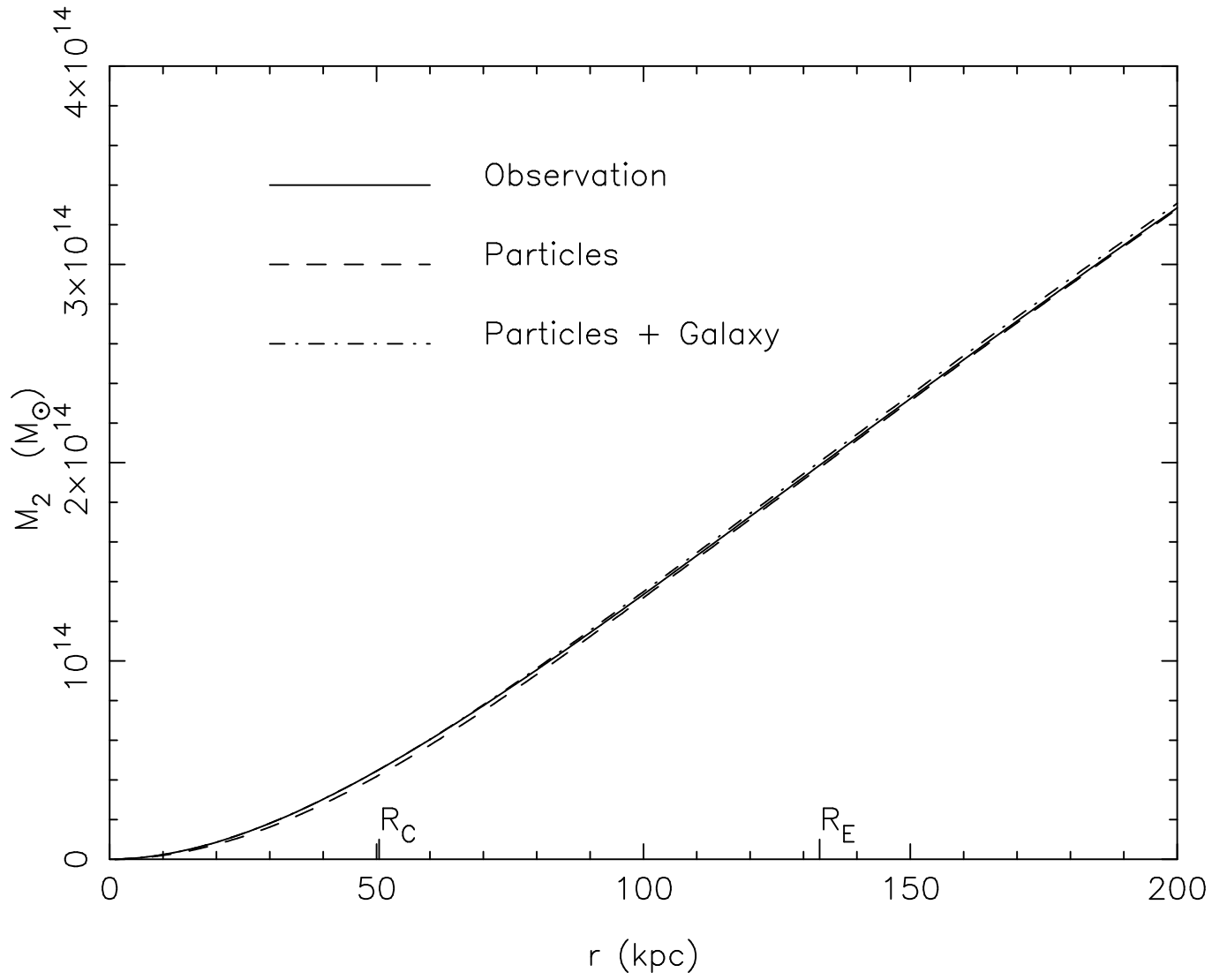


Fig. 8.— 2D encircled mass profiles for massive neutrinos. All three profiles are indistinguishable.

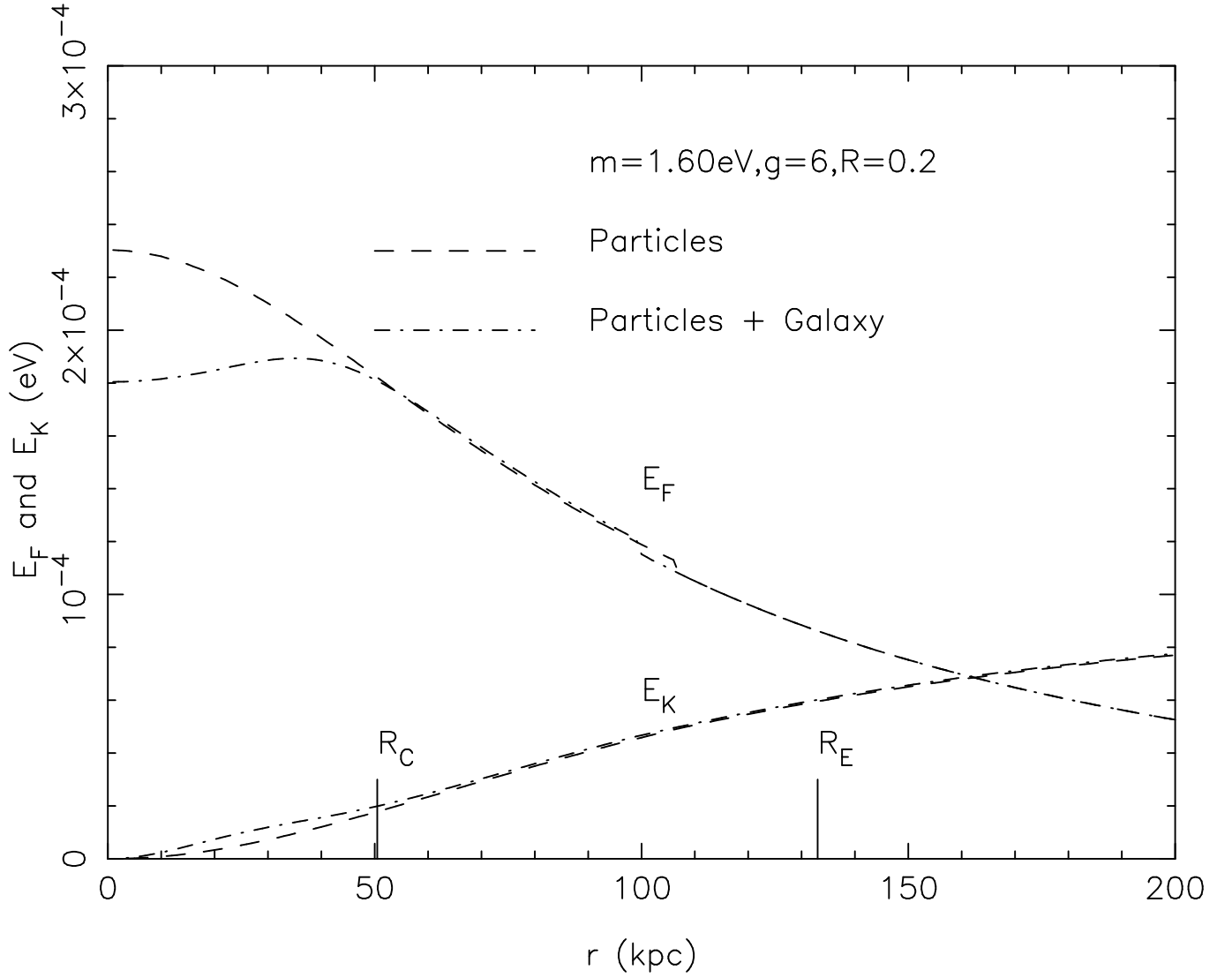


Fig. 9.— Fermi levels and classical kinetic energies of a neutrino for the model without and with the toy galaxy. The model parameters are $m = 1.6$ eV, $g=6$, and $\rho(B)/\rho(DM) = 0.2$. There is a dip of the Fermi level for the model with the galaxy indicating the local softening of the EOS due to the gravity of the galaxy. These energy levels are much higher than those of unbound relic particles of 10^{-7} eV.